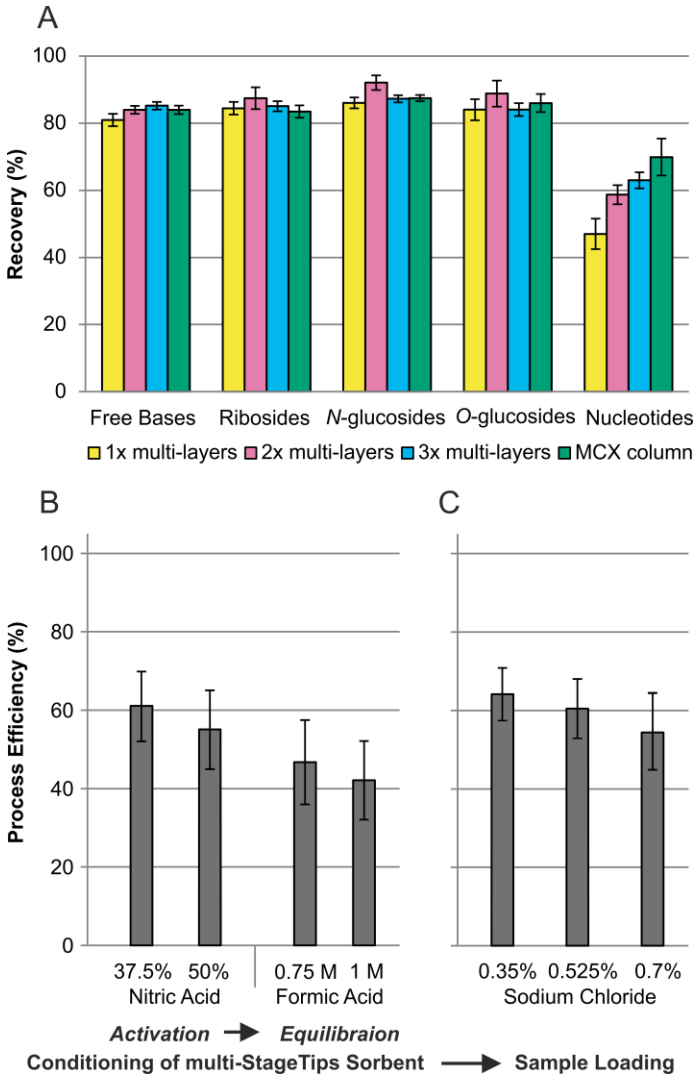

Supplemental Figure 1. Recovery (%) of Different Cytokinin Groups in Relation to the Number of Sorbent Multi-layers (C_{18}/SDB-RPS/Cation-SR) and Total Process Efficiency (%) of In-tip microSPE Protocol.

(A) A number of sorbent multi-layers were tested using a mixture of twenty-six CK standards (0.1 pmol of each). In-tip microSPE compared with a commonly used MCX purification method indicates the usefulness of this method for purification, enrichment and selective compound isolation. Recovery is expressed as the ratio of the mean peak area of an analyte spiked before extraction to the mean peak area of the same analyte standards, multiplied by 100.

(B-C) The conditions for sorbent activation **(B)** and sample loading onto in-tip microSPE **(C)** were optimized to obtain higher yields for all analytes detected. The samples were loaded onto StageTip microcolumns activated by 50% nitric acid or 1 M formic acid using non-diluted/diluted (3:1; 2:1, v/v) solutions of 0.7% NaCl acidified by 1 M hydrochloric acid (pH 2.7) and spiked before extraction with known quantities of the target compounds (0.1 pmol of each CK metabolite). Process efficiency is expressed as the ratio of the mean peak area of an analyte spiked before extraction to the mean peak area of the same analyte standards multiplied by 100. Conditioning with nitric acid and loading of diluted 0.7% NaCl solution (3:1, v/v) were finally used for determination of CKs in isolated protoplasts (see Supplemental Figure 2).

All experiments were performed in quadruplicates and the error bars represent standard error.

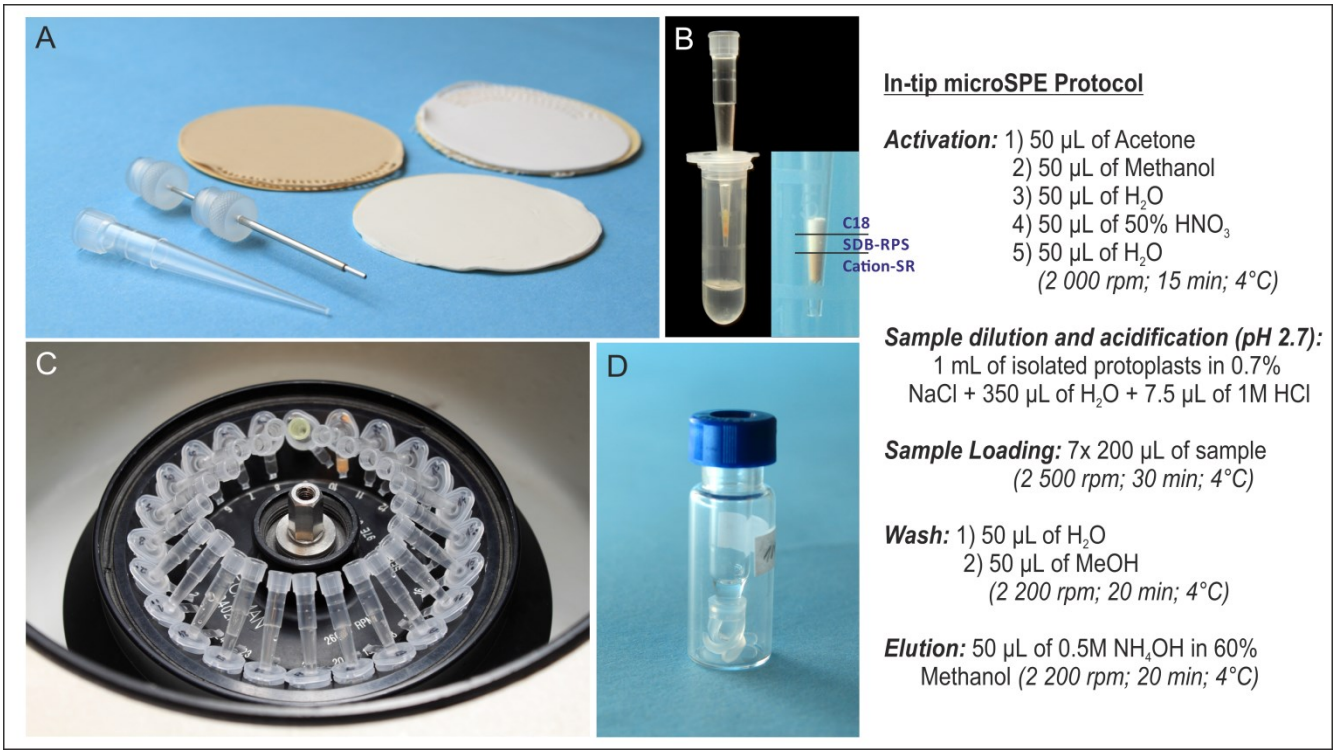

Supplemental Figure 2. Optimized In-tip microSPE Protocol.
Three-layer in-tip µSPE (C18/SDB-RP/Cation-SR) columns were prepared **(A)** and used for purification of isolated protoplasts **(B-C)**. Activation, sample dilution, and loading steps were optimized to obtain higher yields of each analyte measured. The final CK-enriched fraction was evaporated to dryness and dissolved in 40 µL of 10% methanol for LC-MS/MS analysis **(D)**. The description of the optimized protocol is presented at the right-side of the figure. *Photos by Ota Blahoušek.*

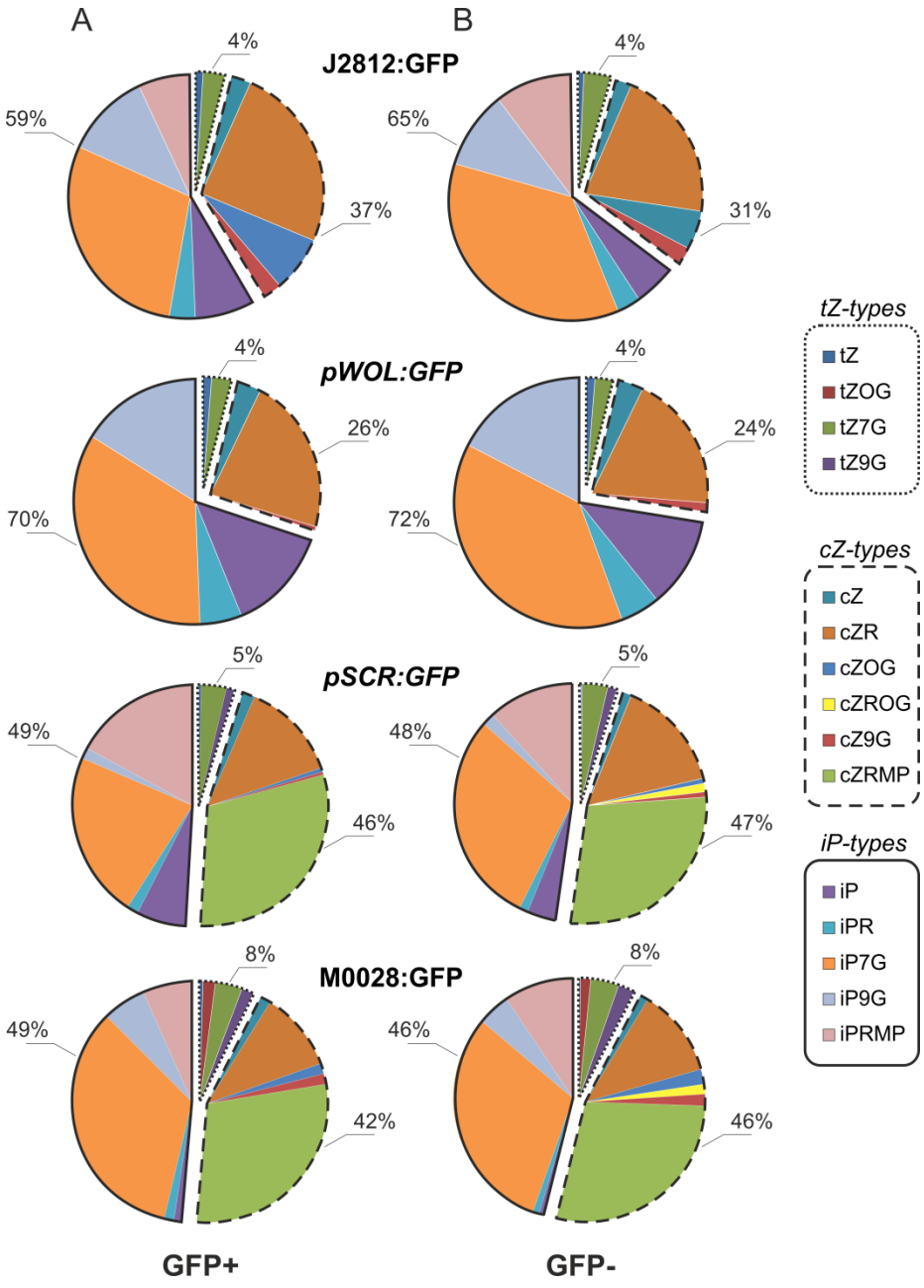

Supplemental Figure 3. Cytokinin Metabolite Patterns in GFP-expressing **(A)** and GFP non-expressing **(B)** Cells of Four Transgenic *Arabidopsis* Lines.

CK distribution of three isoprenoid groups in the isolated protoplast is indicated by different lines (dotted line, *trans*-zeatin-types, *tZ*; dashed line, *cis*-zeatin-types, *cZ*; solid line, isopentenyladenine-types, iP). CK metabolites were quantified in fmol/100,000 protoplasts and the percentages of their distribution were calculated from the sum of the compounds presented. Fifteen CK metabolites were found as follow: the CK nucleotides (iPRMP and *c*ZRMP), the CK ribosides (iPR and *c*ZR), the CK bases (iP, *tZ* and *cZ*), and the CK 7-/9-/O-glucoside conjugates (iP7G, iP9G, *t*Z7G, *t*Z9G, *c*Z9G, *t*ZOG and *c*ZOG). However, *c*ZROG was detected only in the GFP non-expressing cells of the *pSCR:GFP* and M0028:GFP lines.

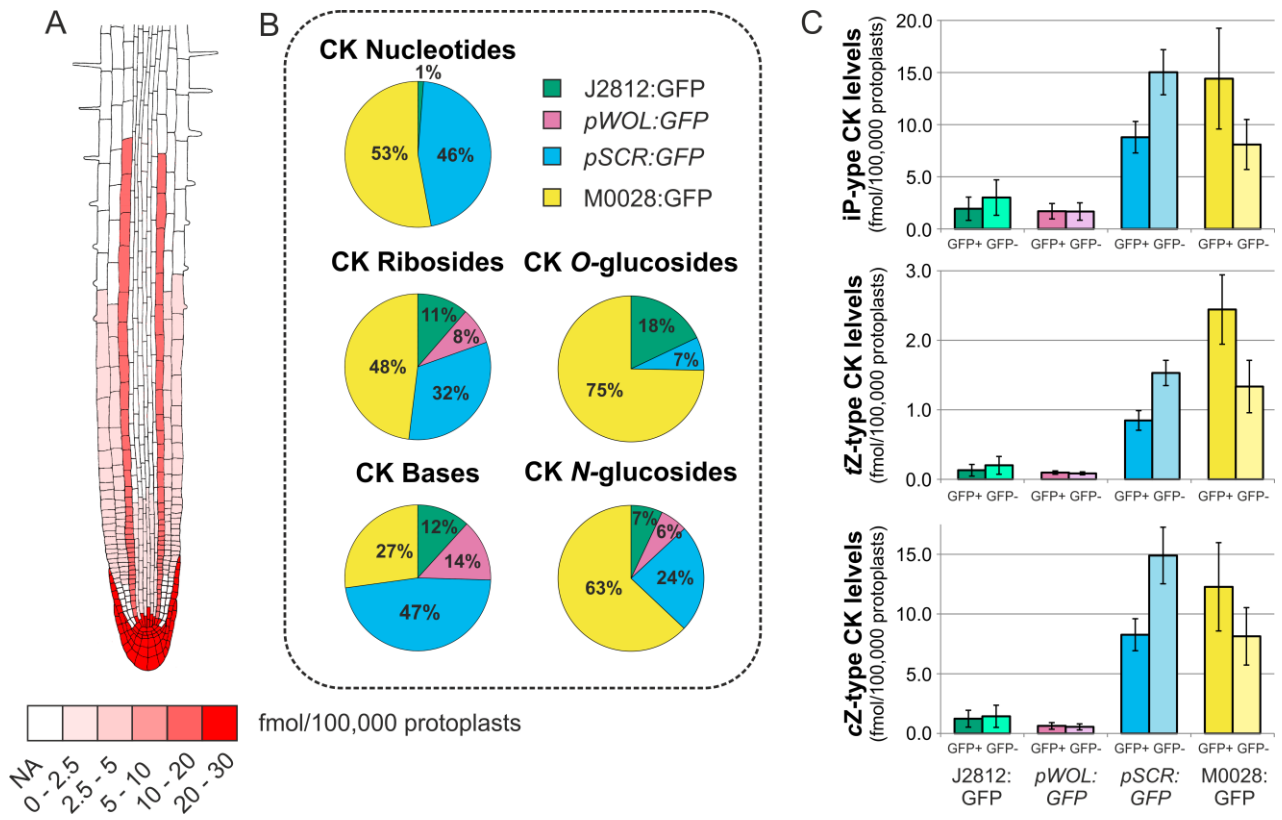

Supplemental Figure 4. Cytokinin Concentration Gradient Exists within the *Arabidopsis* Root Apex.
(A) Cell type-specific CK concentrations were calculated as fmol/100,000 isolated protoplasts, and the total CK concentration in each cell type (according to the J2812:GFP, *pWOL:GFP*, *pSCR:GFP* and M0028:GFP transgenic lines) is indicated by the red colour scale. NA represents the cell populations that were not analysed.
(B) The relative concentration of different CK metabolite groups (nucleotides, ribosides, bases, *O*- and *N*-glucosides) in GFP-expressing cell populations (GFP^+) were calculated from the total levels of each metabolite group.
(C) Total CK levels (in fmol/100,000 protoplast) of three isoprenoid groups detected in the GFP^+ and GFP^- cell types of J2812:GFP, *pWOL:GFP*, *pSCR:GFP*, and M0028:GFP.

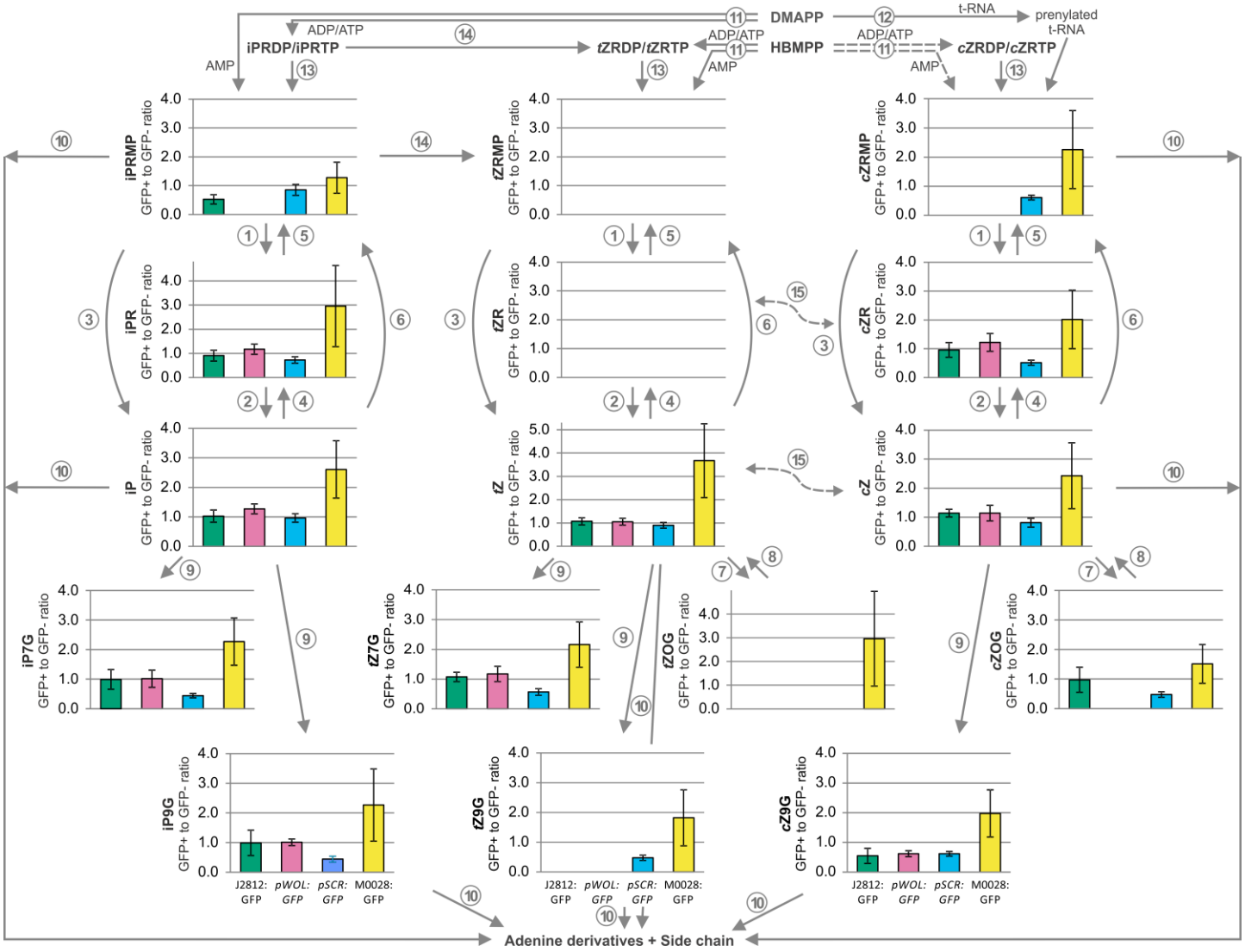

Supplemental Figure 5. Cytokinin Metabolism in Four Different GFP-expressing Cell Populations.
The individual CK metabolites detected in the sorted cell lines are presented. The arrows indicate the CK metabolism and circled numbers denote enzymes involved in CK biosynthesis, interconversions and degradation. (1) 5'-ribonucleotide phosphohydrolase; (2) adenosine nucleosidase; (3) CK phosphoribohydrolase 'Lonely guy'; (4) purine nucleoside phosphorylase; (5) adenosine kinase; (6) adenine phosphoribosyltransferase; (7) zeatin-*O*-glucosyltransferase; (8) ß-glucosidase; (9) *N*-glucosyl transferase; (10) cytokinin oxidase/dehydrogenase (CKX); (11) adenylate isopentenyltransferase (IPT); (12) tRNA-specific isopentenyltransferase; (13) phosphatase; (14) cytochrome P450 mono-oxygenase; (15) zeatin isomerase. DMAPP, dimethylallylpyrophosphate; HMBPP, 4-hydroxy-3-methyl-2-(*E*)-butenyl diphosphate.
The metabolites were quantified in fmol/100,000 protoplasts and the respective ratios were computed in each of the sorted transgenic lines J2812:GFP (green), *pWOL:GFP* (red), *pSCR:GFP* (blue) and M0028:GFP (yellow). The results represent 6 biological replicates and for each 2 technical replicates were performed. Error bars indicate standard error.

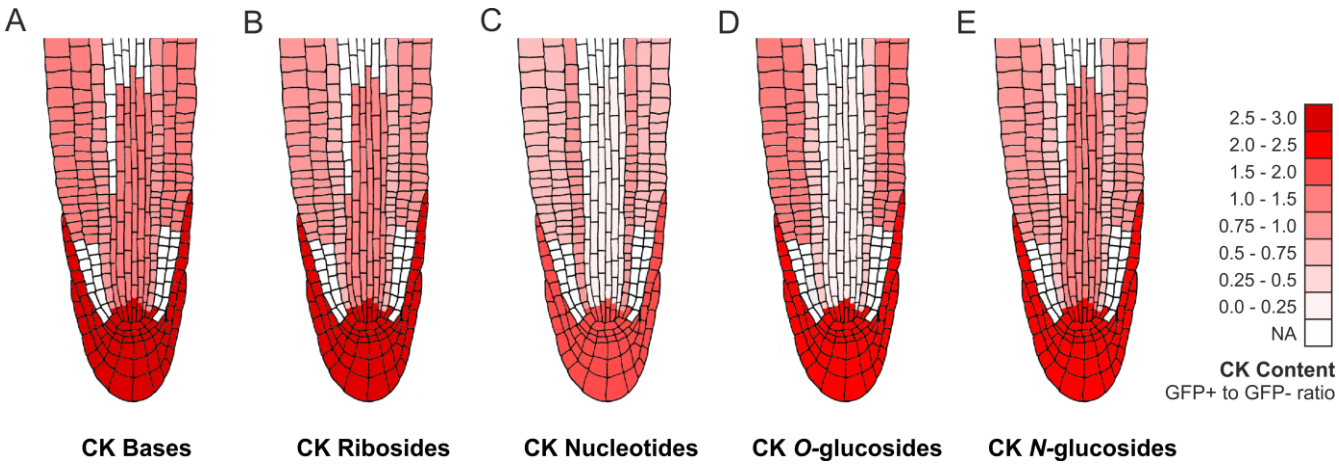

Supplemental Figure 6. Distribution of Cytokinin Metabolite Groups within the *Arabidopsis* Root Tip.
Different patterns of CK bases **(A)**, ribosides **(B)**, nucleotides **(C)**, *O*-glucosides **(D)** and *N*-glucosides **(E)** are present in the stele, the epidermis, and the endodermis and cortex cells. All CK gradient maps showed a concentration maximum in the root cap, columella, columella initials and quiescent centre cells.
The data presented in the maps were derived from 4 GFP lines (J2812:GFP, *pWOL:GFP*, *pSCR:GFP* and M0028:GFP) covering all of the different cell types of the root apex. To compensate for differences in growth and development among the different GFP expressing *Arabidopsis* lines, cell type-specific CK concentrations were calculated in fmol/100,000 isolated protoplasts and then the data were normalized against their respective internal reference GFP^- protoplast populations. The red colour scale indicates the CK content relative to this reference population; NA represents the cell populations that were not analysed; a value of 1 represents CK level in GFP^+ cells equivalent to that in reference GFP^- cells. In the stele, the CK O-glucosides and nucleotides were not detected in either the GFP^+ or the GFP^- cell populations.

Supplemental Table 1. MS optimized conditions.
The precursor and product ions of the studied compounds and optimized collision energies (Fragmentor) are listed. The retention time stability and limits of detection (LOD) are shown for UHPLC-ESI(+)-MS/MS analysis of isoprenoid CKs. Conditions in positive ion mode were as follows: Drying Gas Temperature, 200°C; Drying Gas Flow, 16 L Min^{-1}; Nebulizer Pressure, 35 Psi; Sheath Gas Temperature, 375°C, Sheath Gas Flow, 12 L Min^{-1}; Capillary, 3400 V; Nozzle Voltage, 0 V; Delta iFunnel High/Low Pressure RF, 150/60 V.

Compound	MRM	Fragmentor (V)	Collision Energy (V)	Retention time[a] (min)	LOD[b] (fmol)
*t/c*Z	220.1 > 136.1	380	19	10.15 ± 0.03 / 11.28 ± 0.03	0.1
*t/c*ZR	352.2 > 220.1	380	20	12.92 ± 0.04 / 13.68 ± 0.03	0.1
*t*Z7G	382.2 > 220.1	380	21	7.71 ± 0.01	0.1
t/cZ9G	382.2 > 220.1	380	21	8.93 ± 0.04 / 9.63 ± 0.03	0.5 / 0.1
*t/c*ZOG	382.2 > 220.1	380	21 / 18	9.52 ± 0.01 / 10.35 ± 0.01	0.1
*t/c*ZROG	514.2 > 220.1	380	21	11.96 ± 0.01 / 12.71 ± 0.01	1.0
*t/c*ZRMP	432.2 > 382.2	380	21	8.36 ± 0.02 / 9.01 ± 0.02	1.0 / 5.0
DHZ	222.1 > 136.1	380	23	10.91 ± 0.04	0.1
DHZR	354.2 > 222.1	380	22	13.64 ± 0.01	0.01
(±)DHZ7G	384.2 > 222.1	380	23	8.61 ± 0.01 / 8.92 ± 0.01	0.1
DHZ9G	384.2 > 222.1	380	23	9.61 ± 0.04	0.1
DHZOG	384.2 > 222.1	380	21	10.97 ± 0.03	0.1
DHZROG	516.2 > 222.1	380	22	13.29 ± 0.02	1.0
DHZRMP	434.2 > 384.2	380	23	8.87 ± 0.02	1.0
iP	204.1 > 136.1	380	16	17.88 ± 0.02	0.01
iPR	336.2 > 204.1	380	20	18.15 ± 0.02	0.05
iP7G	366.2 > 204.1	380	21	13.16 ± 0.01	0.1
iP9G	366.2 > 204.1	380	22	16.44 ± 0.02	0.1
iPRMP	416.2 > 204.1	380	22	15.31 ± 0.01	1.0

[a] Values are means ± SD (n = 10). [b] Limit of detection, defined as a signal-to-noise ratio of 3:1.

Supplemental Table 2. List of 107 cytokinin-related genes indicated with their published name and their corresponding accession number.
The genes have been categorized according to their role in CK pathways as Biosynthesis and Metabolism genes **(A)**, Degradation and Conjugation genes **(B)**, Perception and Signaling genes **(C)** and (Candidate) Transport genes **(D)**.

a.	Biosynthesis & Metabolism	
	IPT1	*At1g68460*
	IPT2	*At2g27760*
	IPT3	*At3g63110*
	IPT4	*At4g24650*
	IPT5	*At5g19040*
	IPT6	*At1g25410*
	IPT7	*At3g23630*
	IPT8	*At3g19160*
	IPT9	*At5g20040*
	CYP735A1	*At5g38450*
	CYP735A2	*At1g67110*
	LOG1	*At2g28305*
	LOG2	*At2g35990*
	LOG3	*At2g37210*
	LOG4	*At3g53450*
	LOG5	*At4g35190*
	LOG6	*At5g03270*
	LOG7	*At5g06300*
	LOG8	*At5g11950*
	LOG9	*At5g26140*
	AK1	*At3g09820*
	AK2	*At5g03300*
	APT1	*At1g27450*
	APT2	*At1g80050*
	APT3	*At4g22570*
	APT4	*At4g12440*
	APT5	*At5g11160*

b.	Degradation & Conjugation	
	CKX1	*At2g41510*
	CKX2	*At2g19500*
	CKX3	*At5g56970*
	CKX4	*At4g29740*
	CKX5	*At1g75450*
	CKX6	*At3g63440*
	CKX7	*At5g21482*
	UGT76C1	*At5g05870*
	UGT76C2	*At5g05860*
	UGT73C1	*At2g36750*
	UGT73C5	*At2g36800*
	UGT85A1	*At1g22400*

c.	Perception &Signaling	
	AHK2	*At5g35750*
	AHK3	*At1g27320*
	CRE1/AHK4	*At2g01830*
	AHP1	*At3g21510*
	AHP2	*At3g29350*
	AHP3	*At5g39340*
	AHP4	*At3g16360*
	AHP5	*At1g03430*
	ARR1	*At3g16857*
	ARR2	*At4g16110*
	ARR3	*At1g59940*
	ARR4	*At1g10470*
	ARR5	*At3g48100*
	ARR6	*At5g62920*
	ARR7	*At1g19050*
	ARR8	*At2g41310*
	ARR9	*At3g57040*
	ARR10	*At4g31920*
	ARR11	*At1g67710*
	ARR12	*At2g25180*
	ARR13	*At2g27070*
	ARR14	*At2g01760*
	ARR15	*At1g74890*
	ARR16	*At2g40670*
	ARR17	*At3g56380*
	ARR18	*At5g58080*
	ARR19	*At1g49190*
	ARR20	*At3g62670*
	ARR21	*At5g07210*
	ARR22	*At3g04280*
	CRF1	*At4g11140*
	CRF2	*At4g23750*
	CRF3	*At5g53290*
	CRF4	*At4g27950*
	CRF5	*At2g46310*
	CRF6	*At3g61630*
	CRF7	*At1g22985*
	CRF8	*At1g71130*

d.	Transport	
	ENT1	*At1g70330*
	ENT2	*At3g09990*
	ENT3	*At4g05120*
	ENT4	*At4g05130*
	ENT5	*At4g05140*
	ENT6	*At4g05110*
	ENT7	*At1g61630*
	ENT8	*At1g02630*
	PUP1	*At1g28230*
	PUP2	*At2g33750*
	PUP3	*At1g28220*
	PUP4	*At1g30840*
	PUP5	*At2g24220*
	PUP6	*At4g18190*
	PUP7	*At4g18197*
	PUP8	*At4g18195*
	PUP9	*At1g18220*
	PUP10	*At4g18210*
	PUP11	*At1g44750*
	PUP12	*At5g41160*
	PUP13	*At4g08700*
	PUP14	*At1g19770*
	PUP15	*At1g75470*
	PUP16	*At1g09860*
	PUP17	*At1g57943*
	PUP18	*At1g57990*
	PUP19	*At1g47603*
	PUP20	*At1g47590*
	PUP21	*At4g18205*
	ABCG14	*At1g31770*

Supplemental Table 3. Cytokinin-related gene expression enriched in *pWOL:GFP* **(A)**, M0028:GFP **(B)**, *pSCR:GFP* **(C)** and J2812:GFP **(D)** cell types.
The data derive from GUS and GFP assays and from four transcriptome and proteome studies of cell-specific populations of the *Arabidopsis* root.

A.	***pWOL:GFP* – Stele**
IPT3	[2],[7]
IPT5	[2]
IPT7	[2]
LOG1	[2]
LOG3	[1],[2],[3],[5],[8]
LOG4	[1],[5]
LOG5	[2],[5]
LOG8	[5]
APT3	[8]
CKX5	[9]
CKX6	[2]
UGT85A1	[1],[9]
AHK2	[2]
CRE1/AtAHK4/WOL	[1],[3]
AHP4	[2]
AHP6	[6]
ARR21	[8]
B-ARRs (TCSn:GFP)	[1],[2],[10],[11]
CRF1	[2]
PUP4	[2]
PUP18	[2]
ABCG14	[3]

B.	**M0028:GFP – Lateral root cap, Columella, Columella Initials & QC**
CYP735A2	[4]
LOG1	[3],[8]
LOG8	[5]
APT1	[8]
CKX5	[9]
CKX4	[8],[9]
UGT76C2	[3],[8]
UGT85A1	[2],[3],[8]
B-ARRs (TCSn:GFP)	[11]
CRF6	[3],[8]
ABCG14	[10]

C.	***pSCR:GFP* – Endodermis & QC**
LOG1	[3],[8]
LOG4	[1],[5]
CRF2	[1]
CRF6	[1]
ABCG14	[1]

D.	**J2812:GFP – Epidermis & Cortex**
LOG4	[1]
LOG7	[1],[3],[5],[8]
LOG8	[1]
APT4	[3],[8]
UGT85A1	[1]
ARR8	[3],[8]
CRF2	[1]
CRF3	[1]
ABCG14	[1]

Source:
The *pSCR:GFP* and *pWOL:GFP* lines are in *Arabidopsis* Columbia background (Birnbaum et al., 2003). The J2812:GFP and M0028:GFP lines from the Jim Haseloff GAL4-GFP enhancer trap collections (Jim Haseloff lab, University of Cambridge, http://www.plantsci.cam.ac.uk/Haseloff/) are in *Arabidopsis* C24 background and are available from NASC, the European Arabidopsis Stock Centre, http://arabidopsis.info/ (Stock codes: N9089, N9342).

Supplemental References

[1] **Birnbaum, K. Shasha, D.E., Wang, J.Y., Jung, J.W., Lambert, G.M., Galbraith, D.W. and Benfey, P.N.** (2003). A gene expression map of the Arabidopsis root. Science **302:** 1956–1960.

[2] **Brady, S.M., Orlando, D.A., Lee, J.Y., Wang, J.Y., Koch, J., Dinneny, J.R., Mace, D., Ohler, U. and Benfey P.N.** (2007). A high-resolution root spatiotemporal map reveals dominant expression patterns. Science **318:** 801–806.

[3] **Dinneny, J.R., Long, T.A., Wang, J.Y., Jung, J.W., Mace, D., Pointer, S., Barron, C., Brady, S.M., Schiefelbein, J. and Benfey, P.N.** (2008). Cell identity mediates the response of Arabidopsis roots to abiotic stress. Science **320:** 942–945.

[4] **Kiba, T., Takei, K., Kojima, M. and Sakakibara, H.** (2013). Side-chain modification of cytokinins controls shoot growth in Arabidopsis. Dev. Cell **27:** 452–461.

[5] **Kuroha, T., Tokunaga, H., Kojima, M., Ueda, N., Ishida, T., Nagawa, S., Fukuda, H., Sugimoto, K. and Sakakibara, H.** (2009). Functional analyses of LONELY GUY cytokinin-activating enzymes reveal the importance of the direct activation pathway in Arabidopsis. Plant Cell **21:** 3152–3169.

[6] **Mähönen, A.P., Bishopp, A., Higuchi, M., Nieminen, K.M., Kinoshita, K., Törmäkangas, K., Ikeda, Y., Oka, A., Kakimoto, T. and Helariutta, Y.** (2006). Cytokinin signaling and its inhibitor AHP6 regulate cell fate during vascular development. Science **311:** 94–98.

[7] **Miyawaki, K., Matsumoto-Kitano, M. and Kakimoto, T.** (2004). Expression of cytokinin biosynthetic isopentenyltransferase genes in Arabidopsis : tissue specificity and regulation by auxin, cytokinin, and nitrate. Plant J. **37:** 128–138.

[8] **Petricka, J.J., Schauer, M.A., Megraw, M., Breakfield, N.W., Thompson, J.W., Georgiev, S., Soderblom, E.J., Ohler, U., Moseley, M.A., Grossniklaus, U. and Benfey, P.N.** (2012). The protein expression landscape of the Arabidopsis root. Proc. Natl. Acad. Sci. USA **109:** 6811-6818.

[9] **Werner, T., Motyka, V., Laucou, V., Smets, R., Van Onckelen, H. and Schmülling, T.** (2003). Cytokinin-deficient transgenic Arabidopsis plants show multiple developmental alterations indicating opposite functions of cytokinins in the regulation of shoot and root meristem activity. Plant Cell **15:** 2532–2550.

[10] **Zhang, K., Novak, O., Wei, Z., Gou, M., Zhang, X., Yu, Y., Yang, H., Cai, Y., Strnad, M., Liu, C.J.** (2014). Arabidopsis ABCG14 protein controls the acropetal translocation of root-synthesized cytokinins. Nat. Commun. **5:** 3274.

[11] **Zürcher, E., Tavor-Deslex, D., Lituiev, D., Enkerli, K., Tarr, P.T. and Müller, B.** (2013). A robust and sensitive synthetic sensor to monitor the transcriptional output of the cytokinin signaling network in planta. Plant Physiol. **161:** 1066–1075.